ELSEVIER

Ecological Modelling 148 (2002) 133–151

ECOLOGICAL MODELLING

www.elsevier.com/locate/ecolmodel

An improved cellular automaton model for simulating fire in a spatially heterogeneous Savanna system

Stephen G Berjak, John W Hearne *

School of Mathematics, Statistics and Information Technology, University of Natal, Private Bag XO1, Pietermaritzburg 3209, South Africa

Received 14 February 2001; received in revised form 11 July 2001; accepted 30 July 2001

Abstract

Developments in and around game reserves and ranches in South Africa have led to controlled burning becoming a necessary and regular activity. The management objectives of these fires are well-defined, and thus predicting the duration and extent of a burn is vitally important. Testing scenarios via computer simulation is desirable since this removes the potential risks associated with fire, whilst at the same time ensuring that management policies are attained. There are various approaches to developing a spatial simulation fire model. In this article we present a cellular automaton (CA) model that is capable of predicting fire spread in spatially heterogeneous Savanna systems. The physical basis of Rothermel's fire spread model (1972) was modified to a spatial context and used to improve the CA model introduced by Karafyllidis and Thanailakis (1997). The proposed fire model was verified using data for three human-induced fires in the Mkuze Game Reserve, South Africa, and was found to satisfactorily predict spatial fire behaviour.

Keywords: Fire model; Cellular automaton; Spatial heterogeneity; Mkuze game reserve; Savanna system

1. Introduction

Fire has always played an important role in the development and maintenance of the Savanna communities of Africa (Trollope, 1984a). The need for fire is important since it influences vegetation, in particular grass and tree densities in Savanna (Bond and Van Wilgen, 1996). Consequently controlled burning has become an important rangeland management tool. Thus it is desirable to supplement field experience with computer simulations when deciding where and when a fire should be ignited.

Efforts to model the growth of fires may be classified according to two approaches: vector models and cellular automata (CA) models. Vector models assume that fire burning in an undefined uniform fuel type, spread according to a well-defined growth law, and take a standard geometrical shape such as an ellipse (Kourtz and

* Corresponding author. Tel.: +27-33-260-5626; fax: +27-33-260-5648.

E-mail addresses: sberjak@dip.sun.ac.za (S.G. Berjak), hearne@nu.ac.za (J.W. Hearne).

0304-3800/02/$ - see front matter
PII: S0304-3800(01)00423-9

O'Regan, 1971; Anderson, 1983). If burning conditions are uniform, a single shape can be applied to estimate fire size, area, and perimeter over time, with the use of fractals to account for smaller-scale variations (Finney, 1999). However, most fires do not burn under constant conditions as fuels, weather and topography, vary spatially, and temporally in the case of weather.

More complex vector models use wave propagation techniques, based on Huygen's principle. The principle states that a wave can be propagated from points on its outer edge that serve as independent sources of smaller ignitions, to solve for the position of the fire front at specified times. Models based on this principle require information such as time, direction, and rate of fire spread, for points on the fire edge. The rate of fire spread is estimated by analytical solutions for the propagation of elliptic shape fire perimeters. Consequently wave type models are computationally intensive. Examples of wave-type models developed include Fire Area Simulator (FARSITE) (Finney, 1999) and FIRE! (Green et al., 1995).

CA models, first introduced by Von Neumann (1966), have been successfully used in modelling physical systems and processes. Cellular models for fire growth use fixed distances between regularly spaced grid cells to solve for the fires arrival time from one cell to the next. This approach involves a discrete process of ignitions within the regular structure of a grid-based landscape. There are vanous types of CA models for modelling fire growth, including the transfer of fractional burned area (Karafyllidis and Thanailakis, 1997), probability-driven models (Hargrove et al., 2000) and fractal models (Clarke et al., 1994). Due to the regular lattice structure, CA models provide a useful framework for integrating available spatial data sources and are appropriate for modelling fire spread (Karafyllidis and Thanailakis, 1997).

Karafyllidis and Thanailakis (1997) developed a CA model for predicting fire spread that was applied to hypothetical landscapes under various scenarios of weather and topography. Although the results of their simulations compared favourably with expectations, a thorough investigation of the model revealed certain shortcomings. In particular, whilst the shape of the fire fronts closely resembled the expected shape of fires, the position of the fire front was miscalculated. This was evident in cases involving wind and slope. The source of the problem was the assumption of a scalar field of fire-spread rates (defining the rate of fire spread in any cell in the CA lattice) that was independent of wind and topographic effects. Wind and slope effects were incorporated by weighting the state of the neighbouring cells in the CA local rule depending on the prevailing conditions. Consequently the simulation time step, which was defined in terms of the scalar spread rate only, was miscalculated when wind and slope were introduced as the underlying spread rates were not directly correlated to these factors.

The Karafyllidis and Thanailakis (1997) model also assumed that in a heterogeneous forest, all fuels were combustible - except buildings and water that were allocated zero values for the spread rate. No consideration was given to whether or not a certain fuel type was able to ignite a different fuel type. This simplification was reasonable for the hypothetical forests to which their model was applied. It is not, however, always applicable. For example, fire spreading in grassland may not be sufficiently intense to spread to woodland.

In the next section we attempt to overcome some of the shortcomings of the model by Karafyllidis and Thanailakis (1997). This is done by incorporating the basis of Rothermel's non-spatial fire spread model into a spatial framework.

2. Model formulation

2.1. Description of the model

The fundamental properties of a CA model are the definition of the state of a cell and the local rule that updates this state from one time interval to the next. If the landscape is divided into a matrix of identical square cells and each cell represents a cell in the CA lattice, then the state of (i,j) cell at any time t is defined as a function of the heat dynamics of the cell at that time:

$$S^{t}_{i,j} = f\left(\frac{H_{\mathrm{t}}}{H_0}, t\right) \tag{2.1}$$

where H_t represents the total heat received by the cell from the flame at time t and H_0 is the total heat required to ignite the unburned fuel (calculated at time $t=0$). Consequently, three possible cell states may be deduced from Eq. (2.1).

2.1.1. Unburned cell

This occurs if the fuel in the cell requires additional heating for combustion i.e. $H_t < H_0$. The state of an unburned cell ranges from 0 to 1 depending on the quantity of heat received, where 0 and 1 represent $H_t = 0$ and $H_t = H_0$, respectively.

2.1.2. Burning cell

The fuel in a cell starts burning when sufficient heat has been received to initiate combustion i.e. $H_t = H_0$.

2.1.3. Burned cell

The fuel in a burning cell extinguishes, or is burned, when the heat produced by combustion is insufficient to maintain the combustion process. Each cell in the CA contains parameters describing the fuel characteristics, fuel moisture content and elevation at that particular location. To simplify matters, values for the fuel load (kg m^{-2}), fuel bed depth (m), surface area to volume ratio of the fuel particles (cm^{-1}), extinction moisture content and fuel heat content (kJ kg^{-1}) are assembled into fuel models, which may be selected as needed (Anderson, 1982). As shown in Table 1, natural fuels may be classified according to one of 13 fuel models. The rate of fire spread through a uniform fuel array in the absence of wind and topography, R_0 (m min^{-1}), may then be calculated by applying the values of these parameters in the Rothermel (1972) fire spread equation:

$$R_0 = \frac{I_r \xi}{\rho_b \varepsilon Q_{ig}} \tag{2.2}$$

where I_r is the reaction intensity, which measures the energy release rate per unit area of the fire front (kJ m^{-2} min^{-1}); ξ is the propagating heat flux ratio, which measures the proportion of the reaction intensity that heats the adjacent fuel particles to ignition (dimensionless); ρ_b is the fuel bulk density (kg m^{-3}); ε is the effective heating number, which measures the proportion of a fuel particle that is heated to ignition at the time combustion commences (dimensionless); and Q_{ig} is the heat of pre-ignition, which measures the quantity of heat required to ignite 1 kg of fuel (kJ kg^{-1}). Further details on Eq. (2.2) may be found in Burgan and Rothermel (1984). An advantage of this approach is that Rothermel's model may be used to estimate other parameters frequently required by managers such as fireline intensity, flame length and spotting distance.

In the case of an unburned cell, the rate of fire spread is 0 since no fuel combusts. On the other hand, if the fuel in a cell is burning, then it spreads to the surrounding neighbouring cells at a rate that is a function of R_0, the prevailing wind conditions and the underlying topography. In general, if the (i,j) cell is burning at time t, then the rate of fire spread to the eight neighbouring cells may defined by the vector field:

$$\tilde{R}_{i,j} = R_0 \begin{bmatrix} (\phi_w \phi_s)_{i-1,j} \\ (\phi_w \phi_s)_{i,j+1} \\ (\phi_w \phi_s)_{i+1,j} \\ (\phi_w \phi_s)_{i,j-1} \\ (\phi_w \phi_s)_{i-1,j-1} \\ (\phi_w \phi_s)_{i-1,j+1} \\ (\phi_w \phi_s)_{i+1,j+1} \\ (\phi_w \phi_s)_{i+1,j-1} \end{bmatrix} \tag{2.3}$$

where ϕ_w and ϕ_s are factors that incorporate the effect of wind (speed and direction) and topography on the rate of fire spread, respectively. The product R_0 $(\phi_w\ \phi_s)_{k,l}$ determines the component of the vector velocity field for the rate of fire spread from the (i,j) cell to a neighbouring (k,l) cell.

The rate and pattern of fire spread is significantly influenced by the spatial distribution of fuel. The role of fuel heterogeneity may be incorporated into the CA model by analysing the heat dynamics of the respective fuel classes. A fire will spread from one particular fuel type to another distinct fuel type, if the heat received by the unburned fuel ahead of the flame is sufficient to result in combustion. Expressing this concept

mathematically, a combustibility index CI may be defined as:

$$\mathrm{CI} = \frac{(H_c)_\alpha}{(H_0)_\beta} \tag{2.4}$$

where $(H_c)_\alpha$ represents the amount of heat produced by fuel α that reaches the unburned fuel and $(H_0)_\beta$ is a measure of the total heat required to ignite fuel β. Eq. (2.4) is a slight modification of Eq. (2.1) to facilitate more than one fuel class. If $\mathrm{CI} \geq 1$ then the fire spreads from fuel α to fuel β whereas if $\mathrm{CI} < 1$ then the fire is unable to spread from fuel α to fuel β. The final form of the basic equation for spatial fire spread may be determined by introducing a heterogeneity multiplier, η_f which modifies the rate of fire spread from the (i,j) cell to a surrounding neighbouring (k,l) cell as follows:

$$\tilde{R} = R_0(\phi_w\phi_s)_{k,l}\eta_f \tag{2.5}$$

where the value for η_f is either 0 or 1 depending on the value obtained for CI. If $\mathrm{CI} < 1$, then $\eta_f = 0$, indicating that the fire will not spread from the (i,j) cell to the (k,l) cell. In this case, the rate of fire spread $R_0 = 0$. Similarly, if $\mathrm{CI} \geq 1$ then $\eta_f = 1$, and the fire spreads from the (i,j) cell to the (k,l) cell at a rate determined by Eq. (2.5).

Table 1
Parameters for the standard 13 fuel models developed by Anderson (1982)

Fuel model	Typical fuel complex	Surface-area-to-volume ratio (cm^{-1})/fuel loading (kg ha^{-1})				Fuel bed depth	Moisture of extinction dead fuels
		1 h	10 h	100 h	Live	*m*	Percent
Grass and grass dominated models							
1	Shortgrass(<30 cm)	114/1828	–	–	–	0.305	12
2	Timber (grass and understory)	98/4942	4/2471	1/1235	49/1235	0.305	15
3	Tall grass(75 cm+)	49/7437	–	–	–	0.762	25
Chaparral and shrub fields							
4	High pocosin, chaparral (180 cm+)	65/12379	4/9908	1/4942	49/12379	1.829	20
5	Brush (60 cm)	65/2471	4/1235	–	49/4942	0.610	20
6	Dormant brush, hardwood slash	57/3706	4/6177	1/4942	–	0.762	25
7	Southern rough, low pocosin (60–180 cm)	57/2792	4/4620	1/3706	49/914	0.762	40
Timber litter							
8	Closed timber litter	65/3706	4/2471	1/6177	–	0.061	30
9	Hardwood litter	82/7215	4/1013	1/370	–	0.061	25
10	Heavy timber litter and understory	65/7437	4/4942	1/12379	49/4942	0.305	25
Slash							
11	Lightloggingslash	49/3706	4/11144	1/13615	–	0.305	15
12	Medium logging slash	49/9908	4/34668	1/40845	–	0.701	20
13	Heavy logging slash	49/17321	4/56931	1/69311	–	0.914	25

Heat content = 18610 kJ kg^{-1} for all fuel models.

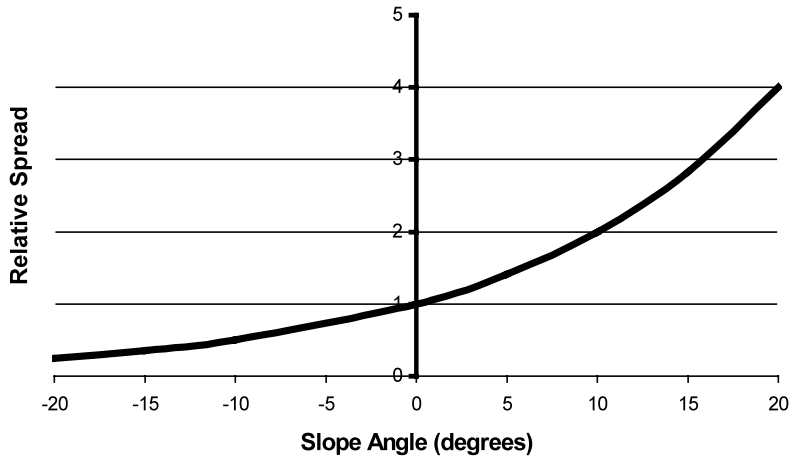

Fig. 1. The effect of slope on increasing or decreasing the rate of spread of the headfire in forests and grasslands.

2.2. Topographic effects

Slope has a considerable influence on the rate of spread, especially in the initial stages of a fire (Luke and Mcarthur, 1978). If a fire burns up a slope, then the angle between the flame and the unburned fuel is reduced. This leads to an increase in the degree of preheating of the unburned fuel immediately in front of the flames, resulting in an increase in the forward rate of spread (Burgan and Rothermel, 1984; Trollope, 1984b; Kushla and Ripple, 1997; Luke and Mcarthur, 1978; Weise and Biging, 1996, 1997). Conversely, the angle increases for a fire spreading down slope and the radiant heat transfer decreases, causing a decrease in the rate of spread.

Data from experimental fires in eucalypt and grass fuels in Australia indicate that the rate of forward progress of a fire on level ground doubles on a 10° slope and increases almost fourfold travelling up a 20° slope (Luke and Mcarthur, 1978). Spread is considerably reduced on down slopes, particularly when moving with the prevailing wind and the general relationship between slope and rate of spread is shown in Fig. 1. In Fig. 1, negative slope angles represent down slope fire spread and similarly, positive angles pertain to up slope spread.

This relationship between spread and slope is generally accepted throughout Australia and is supported by data derived from individual fire reports for the California region by the US Forest Service (Luke and Mcarthur, 1978). Experience gained in the US indicates that the increasing effect of slope on the rate of spread of fires burning uphill doubles from a moderate (0–22°) to a steep slope (22–35°) and then doubles again from a steep to a very steep slope (35–45°) (Trollope, 1984b).

The Australian slope effect is quoted as a multiplying factor of the spread rate. Cheney (1981) proposed the following general relationship between slope and rate of spread:

$$R = R_0 \exp(\alpha \theta_s) \quad (2.6)$$

where R is the rate of spread (m s^{-1}); R_0 is the rate of spread on level ground (m s^{-1}); a is a constant equal to 0.0693; and θ_s is the slope angle (°). Since no quantitative data on the effect of slope on spread rate have been collected in South Africa (Trollope, 1984b), the Cheney (1981) formulation (which was derived for conditions similar to those occurring in South Africa) was applied in our CA model.

In the CA model, each cell contains a parameter for its elevation. The slope may then calculated by finding the difference in elevation between any two neighbouring cells and dividing by the horizontal distance between the two cells. If the cells are adjacent, then the difference in

elevation of the cells is divided by a, whereas for diagonal cells we divide by $\sqrt{2}a$. The angle of the slope, θ_s, may then be calculated by finding the arctangent of the slope.

2.3. Wind effects

Wind is generally viewed as affecting heat transfer from a flame to unburned fuel downwind of the flame primarily by changing the angle between the flame relative to the fuel. Wind increases radiant heat transfer for headfires because the flame is tilted toward the unburned fuel and conversely for backfires (Burgan and Rothermel, 1984; Trollope, 1984b; Luke and Mcarthur, 1978; Nelson and Adkins, 1987; Weise and Biging, 1996, 1997). In many respects, the effect of wind on the rate of fire spread is analogous to that of slope, since both affect the angle between the flame and the unburned fuel.

Flame angle models assess the impact of wind on tilting the flame either toward or away from the surrounding unburned fuel (Weise and Biging, 1996). The flame angle, θ_f, is measured from the vertical in the direction of fire spread. Positive values indicate that the flame is tilted in the direction of fire spread and conversely, negative values indicate that the flame is tilted away from the direction of fire spread.

Numerous authors have derived theory relating flame angle to the ratio of a fire's buoyant force and the force of the horizontal wind. Albini (1981) developed a physical model of the structure of the wind-blown flame of a turbulent wind-driven line fire that included chemical reactions. Putnam (1965) developed a theoretical model relating flame angle to the Froude number defined in terms of the flame length using experimental data for natural gas flames. Nelson and Adkins (1986) examined flame length and angle using data for 22 laboratory and field-scale fires. Weise and Biging (1996) used head fire data to estimate the parameters for both forms of the Froude model.

Fire behaviour studies in South Africa have shown that wind speed has no statistically significant effect on the intensity and flame height of surface grass fires under conditions of controlled burning where wind velocity does not exceed 5.6 m s^{-1} (Trollope, 1984b). Trollope (1978) found that the average height, H_f, of surface head and backfires in grasslands were 2.8 ± 0.4 and 0.8 ± 0.1 m, respectively.

Wills (1987) collected data for 10 field-scale experimental fires conducted in savanna vegetation at the Hluhluwe and Umfolozi Game Reserves in northern KwaZulu-Natal. (Table 2).

Table 2
Conditions of fuel and weather at 10 experimental fires in savanna vegetation in the Hluhluwe and Umlolozi Game Reserves in northern KwaZulu-Natal (from Wills, 1987)

Fuel Moisture		Wind		Slope (degrees)	Rate of spread (m min^{-1})	Flame length (m)
Fire number	Percentage	Speed (km h^{-1})	Direction (degrees)			
HI	4.2	6.3	0	0	7.9	2.0
H2	5.0	12.8	90	0	5.6	1.2
H3	4.4	6.3	0	0	5.0	2.2
H4	4.4	10.1	0	0	17.5	3.0
U1	4.7	13.5	0	0	49.5	3.2
U2	4.8	16.8	0	0	60.1	4.5
U3	4.2	4.2	0	0	2.5	1.0
U4	4.2	12.0	45	0	11.0	2.0
U5	4.2	9.0	0	0	50.0	3.0
U6	4.2	7.2	45	0	9.2	1.5

H = Rluhluwe, U = UmfoIozi.

Table 3
Estimation of β by linear regression with associated correlation coefficient r

	Putnam	Nelson and Adkins	Weise and Biging (flame height model)	Weise and Biging (flame length model)
β	0.0719	0.0835	0.0576	0.0501
r	0.80	0.85	0.87	0.77

These data were used to determine a relationship between the flame angle, produced by the wind, and the resultant rate of fire spread. The flame angle models of Putnam (1965), Nelson and Adkins (1986), Weise and Biging (1996) were applied in this regard. Flame angle models requiring estimates of flame height were implemented assuming a flame height equal to 2.8 m-in accordance with the findings of Trollope (1984b). The earth's gravitational acceleration, g, was approximated as 9.8 m s^{-2}.

The wind factor, ϕ_w was assumed to be an exponential function of the flame angle that modified the rate of fire spread in flat, windless conditions:

$$R = R_0 \exp(\beta\theta_f) \tag{2.7}$$

where $\phi_w = \exp(\beta\theta_f)$ and R_0 was calculated using Eq. (2.2). Taking the natural logarithm of both sides of Eq. (2.7), the value of β for each particular flame model may be estimated by a least-squares linear regression. Table 3 lists the values obtained for β and the correlation coefficient, r, of the predicted versus the observed spread rates. All correlation coefficients were significant at the 5% level.

In the CA model, wind direction is restricted to the eight major compass directions. In referring to directions we assume throughout that the lattice is oriented north–south. The rate of fire spread in the direction of the wind is modified according to the flame angle θ_f. The rate of fire spread in the opposite direction to the wind is adjusted by setting flame angle to $-\theta_f$. In all other directions, the flame angle $\theta_f = 0$. If the wind is diagonally orientated i.e. north east, north west, south east, or south west, then the wind has additional components in the two nearest major compass bearings e.g. a north east wind has components in a northerly and an easterly direction. The magnitude of the wind in these directions is calculated by the cosine of the angle between the wind and the direction of spread. The flame angle in each particular direction may then be calculated based on the respective flame angles. Negative flame angles are applied in the direction directly opposite to the associated wind direction and its components.

2.4. Combined effects of wind and slope

Wind and slope effects may be combined into the rate of spread formula by multiplying their respective components, in a particular direction, using Eq. (2.3). The general form of the equation for a fire spreading from the (i,j) cell to a neighbouring (k,l) cell may be expressed by:

$$\tilde{R}_{i,j} = R_0 \exp(0.0693(\theta_s)_{k,l} + (\beta\theta_f)_{k,l})(\eta_f)_{k,l} \tag{2.8}$$

where the values of θ_f and β depend on the flame angle model in operation. In the absence of wind and on homogeneous, flat terrain, Eq. (2.8) predicts a rate of fire spread $R = R_0$ as expected. The proposed equation for calculating the spread in any direction is adapted into a CA model in the next section.

2.5. Derivation of the CA local rule

The CA local rule determines the influence of the state of a particular cell on some or all of the immediately adjacent neighbours. The neighbourhood of a cell consists of the eight nearest neighbouring cells and the cell itself. The state of the (i,j) cell after a single time step depends on the rate of spread from a neighbouring cell to the (i,j) cell at time t, $R^t_{k,l}$, and the state of the cell itself at time t:

$$S_{i,j}^{t+1} = f(S_{i,j}^{t}, R_{i-1,j-1}^{t}, R_{i-1,j}^{t}, R_{i-1,j+1}^{t}, R_{i,j-1}^{t}, R_{i,j+1}^{t}, R_{i+1,j-1}^{t}, R_{i+1,j}^{t}, R_{i+1,j+1}^{t}) \quad (2.9)$$

Unburned and burned cells (in which no fuel combusts) have spread rates $R_{k,l}^{t} = 0$, and, therefore, have no influence on the state of the (i,j) cell at time t. Cells that are burning have vector spread rates in each direction calculated using Eq. (2.8). The basis for the local rule is derived for conditions in which neither wind nor slope existed. The incorporation of wind and slope factors, as described in the preceding sections, are assumed to modify the rate and pattern of fire fronts generated by the CA model.

To formulate the local rule, let the homogeneous landscape be represented by a matrix of identical cells each with side length a. In the absence of wind and on level ground, the spread rate in each cell is the same and may be calculated using Eq. (2.8) i.e. $R_{k,l}^{t} = R_0$ Furthermore, the total heat required for the fuel in a cell to ignite at time $t = 0$ is represented by H_0. If the (i,j) cell is unburned and only one of its adjacent neighbours is completely burned out, then the (i,j) cell will be completely burned out after a time t_a given by:

$$t_a = \frac{a}{R_{ij}} \quad (2.10)$$

where a is the length of the side of a cell (m) and R is the rate of spread of the fire (m s^{-1}). Similarly, if only one diagonal cell is fully burned out, then the (i,j) will be completely burned out after a time t_d given by:

$$t_d = \frac{\sqrt{2}a}{R_{ij}} = \sqrt{2}t_a \quad (2.11)$$

where $\sqrt{2}a$ is the length of the diagonal of the cell. In this instance, the burning diagonal neighbour will initially spread to two of its adjacent neighbours, which are also adjacent neighbours of the (i,j) cell. Therefore, in the first t_a seconds, the (i,j) cell receives heat from its diagonal neighbour only. Thereafter, additional heat is received from the two common adjacent cells. The rate at which heat is received, per second, by the (i,j) cell is given at any time t is given by:

$$\frac{dH_t}{dt} = \begin{cases} x\left(\frac{H_0}{t_d}\right) & (0 \le t \le t_a) \\ x\left(\frac{H_0}{t_d}\right) + 2\left(\frac{H_0}{t_a}\right) & (t_a \le t \le t_d) \end{cases} \quad (2.12)$$

where x represents the proportion of H_0 that is supplied by the burning diagonal neighbour. Integrating these equations over the time interval $[0, t_d]$ yields:

$$H_t = \int_0^{t_a}\left(\frac{xH_0}{t_d}\right)dt + \int_{t_a}^{t_d}\left[\left(\frac{xH_0}{t_d}\right) + 2\left(\frac{H_0}{t_a}\right)\right]dt = xH_0 + 2H_0\left(\frac{t_d - t_a}{t_a}\right) \quad (2.13)$$

At time $t = t_d$, the sum of the heat received by the (i,j) cell should equal H_0, since the fuel in the cell should commence burning. Applying this condition and substituting Eq. (2.11) for t_d in terms of t_a, we may calculate:

$$H_0 = H_0(x + 2(\sqrt{2} - 1)) \rightarrow x \approx 0.17 \quad (2.14)$$

Thus approximately 17% of the total heat required to burn the (i,j) cell emanates from the neighbouring diagonal cell whereas the remaining 83% is produced by the two adjacent cells (which begin contributing heat at time $t = t_a$). The (i,j) cell is assumed to be burned out at the time when all the surrounding neighbours have commenced burning. In general, if (i,j) cell starts burning at time t_s, then the cell is assumed to burn out after $t_s + t_d$ seconds.

In the presence of wind, topography and heterogeneous fuels, the rate of fire spread to the (i,j) cell varies according to Eq. (2.8). If $R_{k,l}^{t}$, represents the rate of spread from the (k,l) cell to the (i,j) cell at time t, then in a discrete time interval Δt, the CA local rule that updates the cells in the lattice may be given by:

$$S_{i,j}^{t+1} = S_{i,j}^{t} + \left\{\left(\frac{1}{a}\right)(R_{i-1,j}^{t} + R_{i,j-1}^{t} + R_{i,j+1}^{t} + R_{i+1,j}^{t})\right\}\Delta t + 0.17\left\{\left(\frac{1}{\sqrt{2}a}\right)(R_{i-1,j-1}^{t} + R_{i-1,j+1}^{t} + R_{i+1,j-1}^{t} + R_{i+1,j+1}^{t})\right\}\Delta t \quad (2.15)$$

If $S_{i,j}^{t+1} < 1$, then the fuel in the (i,j) cell is unburned and $R_{i,j}^{t+1} = 0$. If $S_{i,j}^{t+1} \geq 1$ and $t < t_s + t_d$, then the fuel in the (i,j) cell is burning and spreads to the surrounding neighbouring cells at a rate calculated by Eq. (2.8). A burning cell is assumed to extinguish at time t if $(t + \Delta t) \geq (t_s + t_d)$. Since no combustion occurs, the rate of fire spread $R_{i,j}^{t} = 0$.

3. Model verification

The model was tested on a number of hypothetical landscapes. Simulations were performed on a 50×50 lattice consisting of square cells with a side length $a = 10$ m. Each cell contained parameters describing its fuel characteristics-fuel load, surface area to volume ratio, fuel bed depth, mean fuel energy content and moisture of extinction-moisture content and elevation. Values for these parameters were assigned according to the scenario implemented, which ranged from fire spreading in a homogeneous landscape on level terrain in the absence of wind, to fire spreading in the presence of a uniform wind, topography and heterogeneous fuels.

3.1. Homogeneous landscapes

Fuel characteristics for an *Acacia nilotica* savanna (Table 4) were assigned to each cell for the scenarios involving homogeneous landscapes. Wills (1987) collected information for this fuel model from the Hluhluwe and Umfolozi Game Reserves situated in northern KwaZulu-Natal. The vegetation of the area is dominated by the grasses *Themeda triandra* and *Cymbopogon excavatus*, and short (up to 2 m) *Acacia nilotica* trees.

Table 4
Fuel model parameters for an *Acacia nilotica* savanna in the Hluhluwe and Umolozi Game Reserves (from Wills, 1987)

Parameters of fuel model for an *Acacia nilotica* Savanna	
Fuel loads	
Fine dead fuel (1 h timelag)	312 g m^{-2}
Medium dead fuel (10 h timelag)	2 g m^{-2}
Live herbaceous fuel	61 g m^{-2}
Live woody fuel	4 g m^{-2}
Surface area to volume ratios	
Fine dead fuel (1 h timelag)	66 cm^2 cm^{-3}
Medium dead fuel (10 h timelag)	3.6 cm^2 cm^{-3}
Live herbaceous fuel	59 cm^2 cm^{-3}
Live woody fuel	59 cm^2 cm^{-3}
Heat content	19500 kJ kg^{-1}
Fuel bad depth	0.44 m
Moisture of extinction	20%

3.1.1. Case 1: no wind and no slope

In the absence of wind and in flat terrain plots of successive fire fronts should produce concentric circles (Byram, 1959; Luke and Mcarthur, 1978; Karafyllidis and Thanailakis, 1997). The model passed this basic test without problem. Results are not presented here but evidence may be seen in the tests that follow.

3.1.2. Case 2: wind and no slope

A choice needs to be made from the four flame angle models discussed in Section 2.3 for incorporation into the CA model. The height of the flame in the Weise and Biging flame height model and the Nelson and Adkins model was set equal to 2.8 m-which corresponded to the average height of grassland headfires recorded by Trollope (1984b). Flame length was assigned in the Weise and Biging flame length model and the Putnam model, according to the values recorded by Wills (1987) for each of the experimental fires (Table 2**).**

A set of simulations for each model was, therefore, performed using fuel and weather data for the 10 experimental fires conducted in the Hluhluwe and Umfolozi Game Reserves. The results are presented in Table 5. The flame height models appear to do a little better than the flame length models. Based on this performance, the remaining simulations involving wind were conducted using the Weise and Biging flame height model.

Fig. 2 illustrates the position of the fire front at 20 min intervals for a fire spreading through a flat, homogeneous landscape in the presence of a northerly wind of 30 m min^{-1}. The simulation time step was 5 s and the fuel moisture content was 1%. The fire was ignited in the centre of the fire fronts.

The rate of headfire spread increased from 2.38 m min^{-1}, in the case of fire spreading with neither wind nor slope, to 3.9 m min^{-1}, whereas the rate of backfire spread decreased to 1.63 m min^{-1}. The

Table 5
Predicted rate of fire spread for each of the flame angle models versus the observed rate of fire spread for 10 experimental fires conducted in the Hiuhiuwe and Umfolozi Game Reserves by Wills (1987)

Case	Observed (m min^{-1})	Weise and Biging (flame height) (m min^{-1})	Nelson and Adkins (m min^{-1})	Putnam (m min^{-1})	Weise and Biging (Flame length) (m min^{-1})
HI	7.9	8.8	85	10.0	11.0
H2	5.6	1.4	1.4	1.4	1.4
H3	5.0	9.0	8.5	9.5	10.3
H4	17.5	20.0	20.0	17.0	17.0
U1	49.5	30.7	40.0	24.0	24.0
U2	60.1	40.0	60.0	30.0	24.0
U3	2.5	5.2	4.8	9.5	10.0
U4	11.0	15.0	15.0	17.0	17.0
U5	50.0	17.0	15.5	13.0	15.0
U6	9.2	6.8	6.2	9.5	10.0
r	–	0.88	0.85	0.79	0.78

shape of successive fire fronts is an approximate ellipse with the long-axis parallel to the direction of the wind as expected (Anderson, 1983; Byram, 1959; Luke and Mcarthur, 1978).

The effect of wind on transforming the shape of the fire front from a circle-in the case of no wind-to an ellipse, where the degree of elongation depends on the wind speed, was a commonly observed phenomenon in all simulation tests. Fons (1946) found that the shape of the burned area in any fuel type is independent of the compactness and fuel moisture content. He confirmed this by comparing the means of the ratio of angular spread distance to the maximum spread distance obtained within each wind class for the upper and lower ranges of compactness and moisture content (Anderson, 1983). This analysis ascertained that the shape of the burned area was dependent upon wind velocity only, and led to the formulation of an equation for the ratio of maximum length-to-width for mat beds of ponderosa pine needles as a function of the wind velocity.

To determine the influence of fuel moisture on the rate and pattern of fire spread, simulations were conducted using a flat, homogeneous landscape in which the fuel moisture contents were assumed to be 1, 5 and 10% with uniform wind velocities ranging from 0 to 200 m min^{-1}. In accordance with Fons (1946) findings, the length-to-width ratio of the fire fronts produced by the CA model was found to vary with the wind speed only and was independent of the moisture content of the fuel. Fig. 3 is a graph of the length-to-width ratio versus the wind speed for a homogeneous landscape with fuel moisture content of 1, 5 and 10%.

An explicit function for the length-to-width ratio (l/w) of a fire in terms of the wind velocity (U)

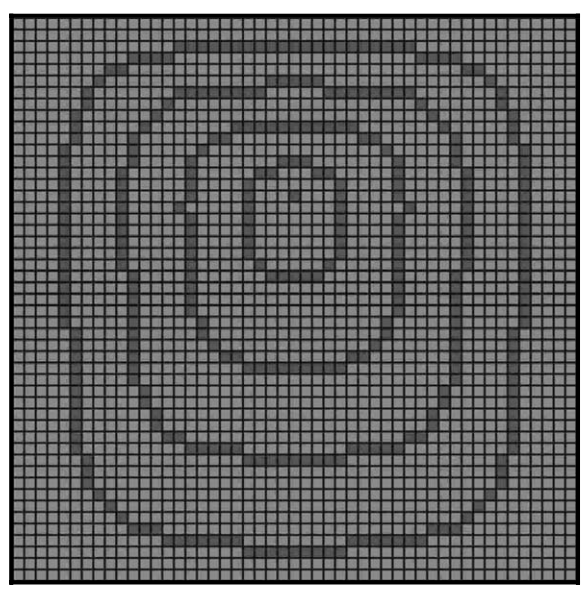

Fig. 2. Fire fronts in a flat, homogeneous landscape with a northerly wind of 30 m min^{-1}. The fire is ignited at the centre of the fire fronts that are displayed at 20 min intervals.

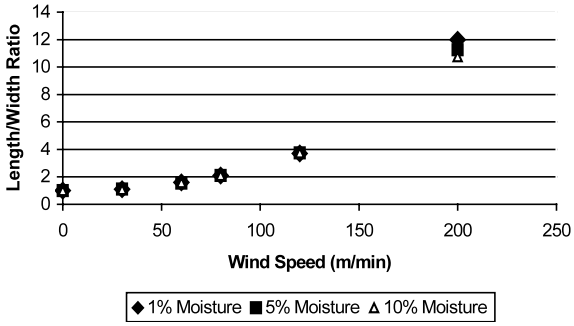

Fig. 3. Wind speed versus length-to-width ratio for a fire spreading in a homogeneous landscape with fuel moisture content of 1, 5 and 10%.

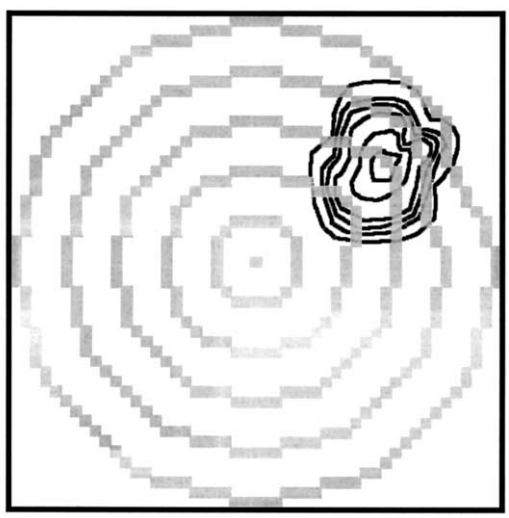

Fig. 4. Fire spreading in a homogeneous forest containing a hill or mountain in the absence of wind. The topographical feature is represented by the black contour lines that are at 2 m intervals. Successive fire fronts are displayed at 20 min intervals.

measured in m min^{-1} was calculated via a least-squares regression of the simulation results as:

$$\frac{l}{w} = 0821\exp(0.0127U) \quad (3.1)$$

with a correlation coefficient $r = 0.99$, which is significant at the 1% level. Eq. (3.1) is useful for predicting the dimensions of a fire spreading through a homogeneous fuel in the presence of a constant wind.

3.1.3. Case 3: slope and no wind

Fig. 4 depicts the passage of a fire front spreading in a homogeneous landscape containing a hill or mountain. The topographical feature is represented by the black contours to the north east, which are displayed at 2 m intervals. The fire spreads in the absence of wind and successive fronts are displayed at 20 min intervals. The fuel moisture content was set to 1% to maintain consistency with previous simulations and facilitate comparison of results. In the first 20 min, the fire spreads in a circular fashion at approximately 2.38 m min in all directions. Upon encountering the hill, the rate of spread in that direction increases, since the fire is burning up the slope. The rate of spread in all other directions, however, remains unchanged. The first evidence of the increased rate of spread occurs after 40 min as the shape of the fire front becomes more pronounced in the north east. The rate of spread up the hill is approximately 4.12 m min^{-1}.

After an hour the fire reaches the summit and begins to descend the hill. As the fire spreads down the slope, the rate of spread decreases to roughly 1.5 m min^{-1}, resulting in the retardation of the front in that direction. After 100 min has elapsed, the fire passes the hill and commences spreading on level terrain.

As a consequence of the topographical feature, the overall shape of the fire is slightly distorted in the north east direction. The net effect of the hill has caused the fire to spread more slowly in that particular direction compared with all other directions, thus resulting in non-circular fire fronts.

In conclusion there is good agreement between the behaviour of the model and expected fire behaviour as reported in the literature (Luke and Mcarthur, 1978; Trollope, 1984b; Weise and Biging, 1997).

3.2. Heterogeneous landscapes

To incorporate the effect of heterogeneity into the model, a second fuel model was introduced. The fuel characteristics represented a Highland Sourveld consisting of a 2-year-old *Themeda triandra* grassland. The information describing this fuel model was collected by Everson et al. (1988)

for the KwaZulu-Natal Drakensberg and is displayed in Table 6.

Note that grasslands do not contain woody plants or coarse dead fuel (10, 100 and 1000 h timelag) and, therefore, these components do not appear in Table 6.

Fig. 5 shows the simulation results for a fire spreading through a heterogeneous landscape containing fuel for an *Acacia nilotica* savanna and a Highland Sourveld grassland. The fuel moisture content of the former was assigned a value of 1%, which was the same as in all previous tests, and the latter was assigned a relatively high value of 8%.

Table 6
Fuel model parameters for a Highland Sourveld grassland in the KwaZulu-Natal Drakensberg (Everson et al., 1988)

Parameters of fuel model for a Highland Sourveld Grassland	
Fuel loads	
fine dead fuel (1 h timelag)	336 g m^{-2}
Live herbaceous fuel	224 g m^{-2}
Surface area to volume ratios	
Fine dead fuel (1 h timelag)	66 cm^2 cm^{-3}
Live herbaceous fuel	49 cm^2 cm^{-3}
Heat content	19990 kJ kg^{-1}
Fuel bad depth	0.305 m
Moisture of extinction	30%

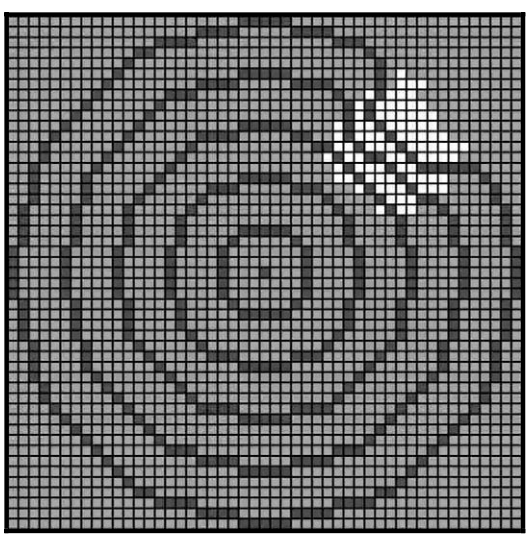

Fig. 5. Fire spreading in a heterogeneous landscape with neither wind nor slope. Grey cells represent an *Acacia nilotica* savanna, with a moisture content of 1%, and white cells a Highland Sourveld grassland, with a moisture content of 8%. Successive fronts are displayed at 20 min intervals.

In the first 40 min, the fire spreads through the *Acacia nilotica* savanna in a circular pattern at approximately 2.38 m min^{-1}. After an hour, the fire reaches the Highland Sourveld grassland in the north east. Since the fire is sufficiently intense to ignite the grassland fuel, it continues to spread in this direction. The rate of spread, however, decreases as the fire passes through the grassland to approximately 1.1 m min^{-1}. In all other directions the rate of fire spread remains constant.

As a consequence of the reduced rate of spread, the fire fronts become non-circular and begin to bend in the region of the grassland. The effect of heterogeneity, with respect both fuel composition and moisture content, is very pronounced after 100 min, as the fire spreads even more rapidly through the savanna vegetation than the grassland. This is due to the relatively high moisture content of the grassland compared with the savanna.

A second scenario was tested in which the fuel moisture content of the grassland was increased to 20%. The objective of this simulation was to determine the effect of an increase in the level of heat required for combustion of the grassland fuel. The simulation was implemented using the same parameter settings as the previous example, except for the fuel moisture content of the grassland. The fire spread in the same manner through the savanna as previously described. However, it was unable to ignite the fuel in the grassland. This resulted in the fire fronts bending around the region occupied by the grassland while continuing to spread at a constant rate in all other directions.

A further scenario was implemented to determine the influence of the wind on the rate and pattern of fire spread in a heterogeneous landscape. The fuel moisture content of the savanna and the grassland were 1 and 20%, respectively, as in the previous example. In the first 40 min the fire spread in the absence of wind and successive fire fronts remained unchanged from the previous two simulations. Thereafter, a gentle southwest-

erly breeze of 30 m min^{-1} was introduced. The subsequent increase in heat supplied from the savanna fuel, resulting from the presence of the wind, facilitated fire spread into the grassland fuel producing a qualitatively similar result to that presented in Fig. 5. In contrast, reducing the initial wind speed from 30 to 20 m min^{-1} resulted in the inability of the fire to spread into the grassland.

The model has been implemented to hypothetical landscapes under various scenarios of fuel, wind and topography, and both the rate and pattern of fire spread predicted by the model is in good agreement with experience. In practice, however, the response of a fire is not easily isolated to individual changes in wind, topography and heterogeneous fuel. Rather, it is the collective influence of these spatially varying parameters that account for the properties of the fire. In the next section the model is used to simulate actual fire events that occurred in Mkuze Game Reserve (MGR) during 1997.

4. Case study

4.1. Mkuze game reserve

Mkuze Game Reserve (MGR) is one of the large reserves managed by the KwaZulu-Natal Nature Conservation Services. Located in northern KwaZulu-Natal and covering an area of approximately 37 000 ha (Fig. 6), MGR has an exceptionally high bio-diversity comprising flora and fauna (Goodman, 1982).

At MGR, both lightning and man-induced fire is believed to have played a major role in the development of the vegetation of the area and fire is currently used on a regular basis as a management tool. According to Goodman (1990) the primary objectives of this are to:

- maintain or enhance spatial heterogeneity.
- Ensure fodder flow to large mammals.
- Retard woody plant growth.
- Reduce the risk of accidental or arson fires that will threaten the survival of plant species or destroy the composition or structure of a priority vegetation community.

The decision to ignite vegetation should consider whether the resultant fire will achieve the desired effect, while still remaining in the required limits of safety. Consideration of the many factors influencing fire behaviour together with a great deal of experience is involved in making the decision as to where and when a fire should be started. It is felt that a simulation model could provide very useful additional information before such a decision is made.

The model was implemented using the information for the Mahlabeni region of MGR. The performance of the model was assessed by comparing the areas (total, overlapping, underestimation, overestimation) of the fire boundary produced by the model with the actual fire boundary. Information contained in the fire record (documented by reserve management) indicates that the fire was ignited at 13:00 h in the presence of a light, north easterly breeze and the fire continued to burn until its extinction at 18:00 h that evening. At around 15:00 h, the wind ceased. Table 7 summarises the initial parameter values used for the simulation.

4.2. Fuel layer

The vegetation of the entire reserve was mapped to the 13 fuel models of Anderson (1982), plus two non-fuel classes. The fuel class layer was generated from a single scene of Landsat Thematic Mapper (TM) imagery using a combined supervised/unsupervised approach (Congalton et al., 1993; Thompson, 1993). Image classification was enhanced through the use of aerial photography and ancillary GIS data layers. The latter included a detailed vegetation coverage containing fields for vegetation physiognomy, floristics, sensitivity/conservation value, soils and geology (Goodman, 1990).

The vegetation in the Mahlabeni region (Fig. 7) was dominated by a short grass covering (fuel model 1) and to a lesser extent tall grass (fuel model 3), timber-grass and understory (fuel model 2), chaparral (fuel model 4) and heavy timber litter (fuel model 10). The final extent of the prescribed patch burn was recorded using a global positioning system (GPS) and then captured into a GIS.

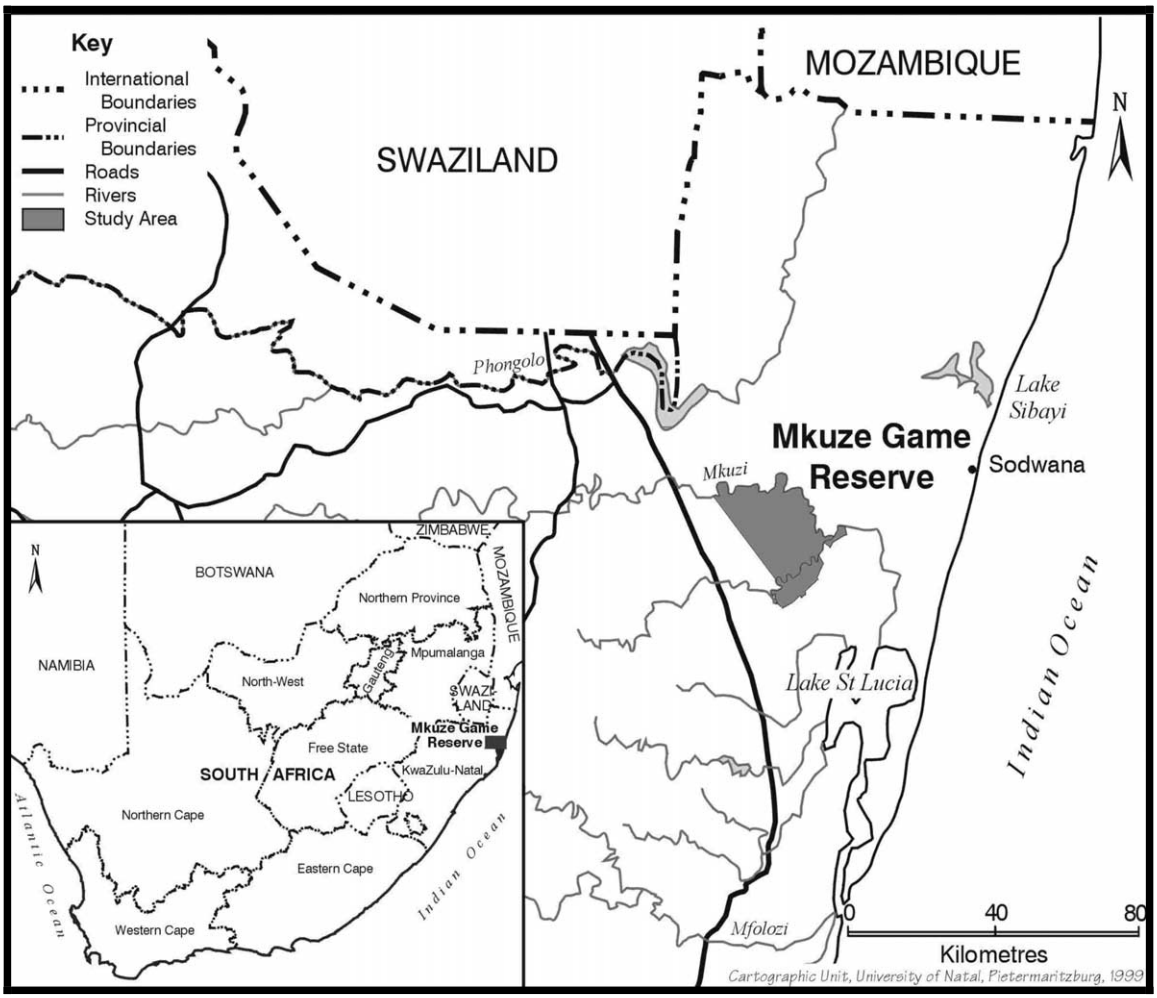

Fig. 6. Location of MOR, KwaZulu-Natal, South Africa.

Table 7
Summary of initial parameter values for simulating Mahlabeni fire

Fuel moisture				
Wind speed	Wind direction	content (all fuels)	Cell size	Simulation time step
30 m min^{-1}	North East	1%	25×25 m	60 s

4.3. Topographic layer

Fig. 8 shows 5 m interval contours of the Mahlabeni region. Vector contours for the majority of MGR were captured into a GIS at a 5 m interval and used to generate a 25×25 m digital elevation model (DEM) of the entire reserve. The topography of the burned region was characterised by gradual slope that increased in a south easterly to northwesterly direction. The highest

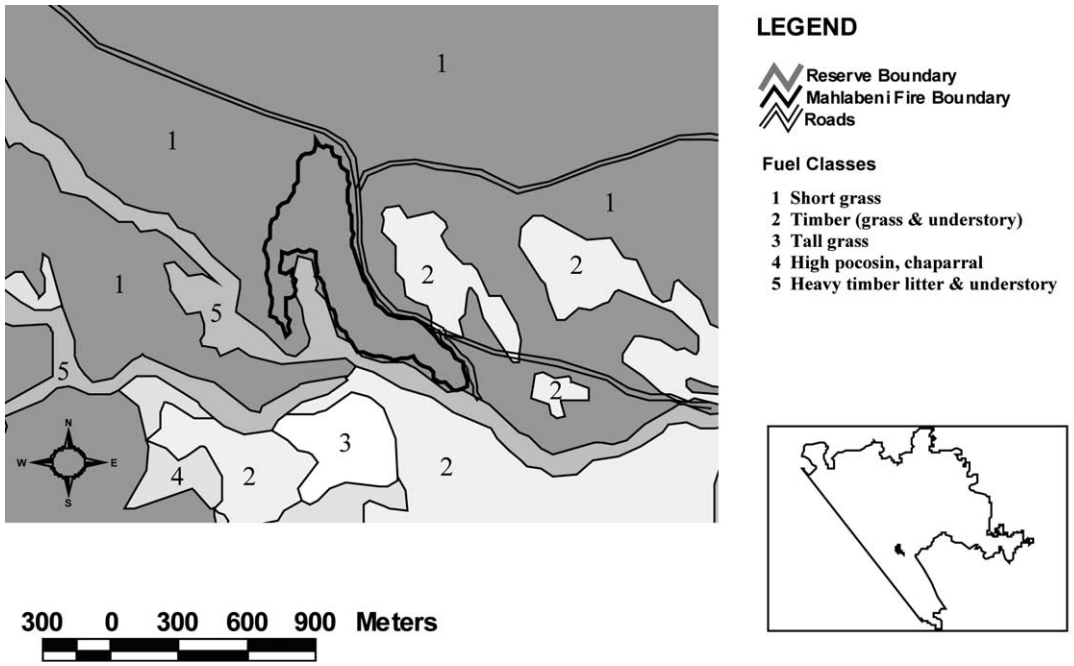

Fig. 7. Map of fuel classes and final extent of a prescribed patch burn.

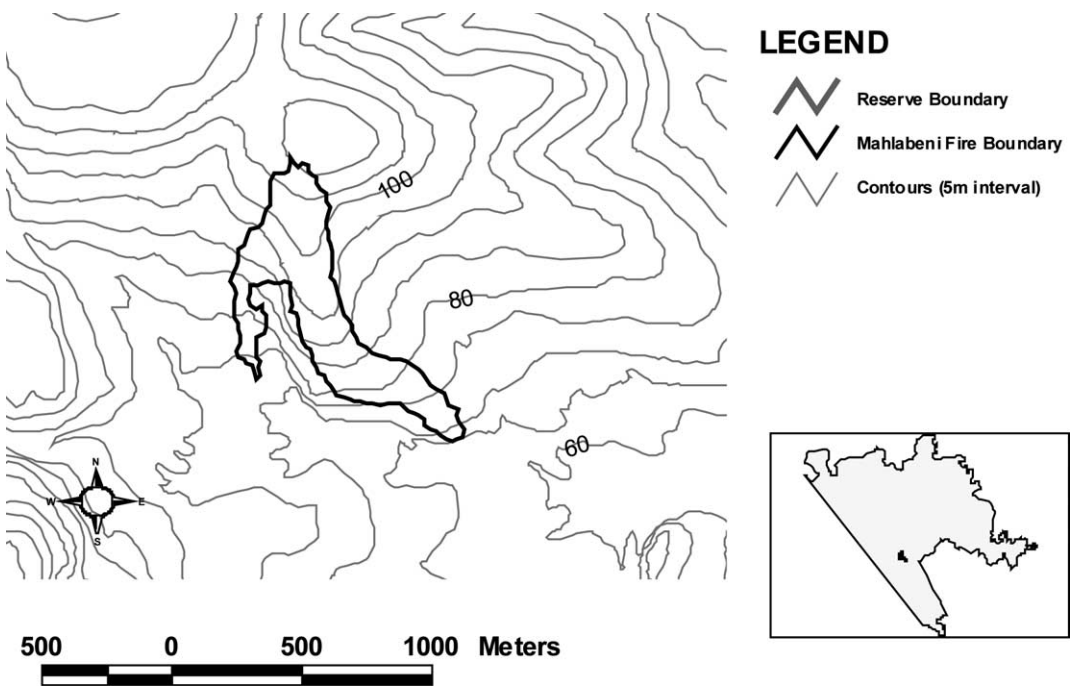

Fig. 8. Contours at 5 m intervals of a prescribed patch burn.

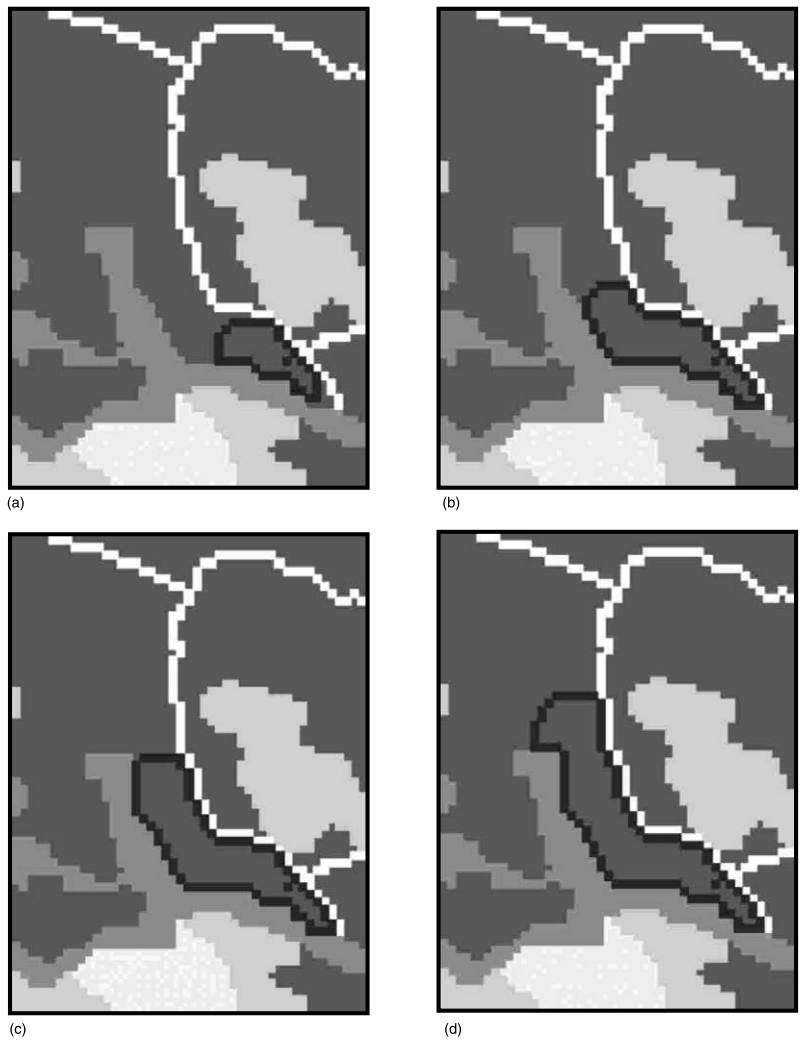

Fig. 9. Fire fronts generated by the simulation model for the Mahlabeni area of MGR displayed after (a) 1 h, (b) 2 h, (c) 3 h, (d) 4 h.

and lowest points corresponded to the base of the valley (65 m) and the top of the hill (110 m), which translates into an approximate gradient of 1 in 28 or a 2°-slope angle.

4.4. Simulation results

Fig. 9 is a graphical representation of the fire fronts, displayed at 1 h intervals, produced by the simulation model, for the Mahlabeni fire. In the first 3 h, the fire spread in the presence of a light northeasterly breeze of 30 m min^{-1}. The rate of spread up the slope, i.e. from the southeast to the northwest, after 1 h was approximately 3.9 m min^{-1}, whereas the downslope spread rate was only 2.4 m min^{-1} (Fig. 9(a)). The rate of head and backfire spread was restricted by the heavy timber litter and understory and the road, respectively.

The fire maintained an uphill spread rate between 3.7 and 4.1 m min^{-1} for the next couple of hours. After 3 h had elapsed on the simulation clock, the wind ceased. This was accounted for by reducing the wind speed to 0. This alteration had

little effect on the spread rate up the slope be-tween the third and fourth hours, which remained at 3.6 m min^{-1} (Fig. 9(c) and (d)). This follows expectation as the fire spreading in a northwest direction is influenced primarily by the gradient of the slope rather than the wind, which is blowing at right angles to the slope.

At around 18:00 h, 5 h after ignition, the fire (at the field site) had extinguished itself. Goodman (personal communication, 1999) attributed the fire's extinction to the formation of dew on the ground resulting from a decrease in the air temperature in the late afternoon and early evening. Luke and Mcarthur (1978) found that dew might contribute to the moisture content of plants and have the effect of delaying the start of fires. The reduction in the air temperature and the formation of dew was incorporated into the model by systematically increasing the fuel moisture content of all unburned fuels.

For the Mahlabeni fire, the air temperature was assumed to start decreasing at 17:00 h. Consequently, the moisture content of the short grass, which carried the fire, was increased from its initial value of 1–3% after 4.25 h had elapsed on the simulation clock or 17:15 h real time. Thereafter, the moisture content of the short grass was increased linearly, by 3% every 15 min. At 18:00 h the moisture content reached the extinction level of 12% resulting in the 'burn out' of the fire (Fig. 10).

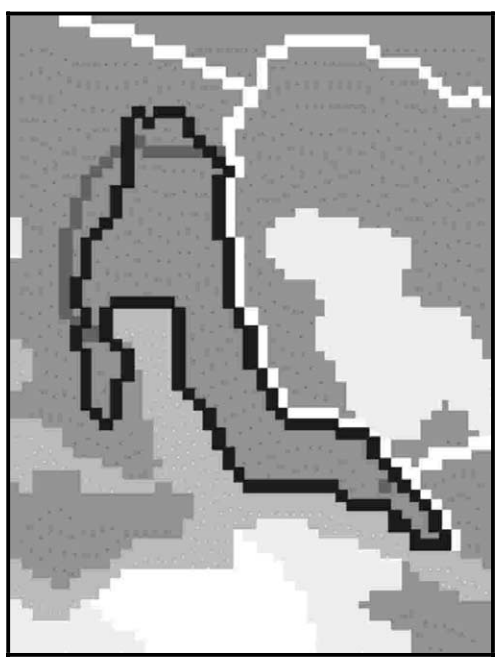

Fig. 10. Fire boundary after 5 h generated by the simulation model compared with the observed fire boundary (black cells) for the Mahlabeni area of MGR.

Comparison of the location of actual area burnt (26 1250 m^2) with the simulated burn revealed that 81% of the area corresponded. The simulated burn included an area of 12% not burnt in the field (overestimation) and 7% burnt in the field but not in the simulation (underestimation). Two further simulations were performed corresponding to actual fires that occurred in the Mahlala and Khongolwane areas of MGR. The simulated Mahlala fire burnt an area of 89% in common with the actual fire with a 7% underestimate and 4% overestimate. Fire was started at two distinct points in the case of the Khongolwane fire but the eventual burn formed a continuous area. For this fire 88% of the simulated burn overlapped with the actual area burnt with a 12% underestimate and no overestimate.

5. Conclusion

An improved spatial model for predicting fire dynamics in savanna ecosystems has been developed. One of the main advantages this CA model enjoys over vector-based models is the ease with which GIS and other spatial data can be used. The extent of computational effort is another big advantage. Karafyllidis and Thanailakis (1997), Hargrove et al. (2000) are two of the most recent models also enjoying these advantages. The latter model was designed for broader temporal and spatial scale than required for the purpose of this project. The model by Karafyllidis and Thanailakis (1997), on the other hand, was found to be flawed for certain situations.

The starting point in the formulation of our model is the physical basis of Roffiermel's model (1972, 1983). The effect of wind on the rate and pattern of fire spread was incorporated by examining various flame angle models, using empirical data for fires in the Hluhluwe and Umfolozi

Game Reserves. The model that best approximated these data was then integrated into a CA model. Spatial fuel heterogeneity was incorporated into the CA model by analysing the heat dynamics of the respective fuel components.

Implementation of the proposed model to hypothetical landscapes under various scenarios generated fire fronts that were found to be in good agreement with observed experience of fire spread. The model was also applied to three actual fire events using information collected for prescribed burning operations conducted in MGR during 1997. In all three cases the rate and pattern of simulated fire boundaries showed favourable agreement with the observed fire boundaries. The model accounted for the critical elements governing fire spread including wind, topography and fuel heterogeneity. Inherent characteristics of the simulation model included the prediction of fire containment, by physical constructs such as roads and natural barriers (for example vegetation), and backfire extinction. Reproduction of fire boundaries facilitated an improved understanding of the fire system and its controlling factors.

The fire growth model has the potential for integration with existing models used in ecosystem management including models of bush encroachment and plant–herbivore dynamics and thus the holistic management of savanna systems.

Acknowledgements

The authors would like to acknowledge the contribution of Joe Schiller of the Satellite Application Centre (SAC) for kindly donating the Landsat TM imagery and Dr Peter Goodman of the KwaZulu-Natal Nature Conservation Services for his valuable input throughout the project. Funding from the South African National Research Foundation and the University of Natal is gratefully acknowledged.

References

Albini, F.A., 1981. A model for the wind-blown flame from a line fire. Comb. Flame 43, 155–174.

Anderson, H.E, 1982. Aids to determining fuel models for fire behaviour, USDA For. Serv. Intermt. For. Range Exp. Stn. Ogden, UT. Gen. Tech. Rep., INT-122: pp. 22.

Predicting wind driven wild land fire size and shape. USDA For. Serv., Intermt. For. And Range Exp. Ogden, UT. INT-305: pp. 26.

Bond, W.J, Van Wilgen, B.W., 1996. Fire and plants. In: Population and Community, Biology, vol. 14. Chapman and Hall, London, pp. 188–203.

Burgan R.E, Rothermel, R.C, 1984. BEHAVE: Fire behaviour prediction and fuel, modelling system-Fuel subsystem. USDA For. Serv., Intermt. For. and Range Exp. Stn., Ogden, UT. Gen. Tech. Rep. INT-167: pp. 126.

Byram, G.M., 1959. Combustion of forest fuels. In: Davis, K.P. (Ed.), Forest Fire—Control and Use. McGraw-Hill, New York, pp. 61–89.

Cheney, N.P., 1981. Fire behaviour. In: Gill, A.M., Groves, R.H., Noble, I.R. (Eds.), Fire and the Australian Biota. Australian Academy of Science, Canberra, pp. 157–175.

Clarke, K.C., Brass, J.A, Riggan, P.J., 1994. A cellular automaton model of wildfire propagation and extinction. Photogrammetric Eng. Remote Sensing 60 (11), 1355–1367.

Congalton, R.G., Green, K, Teply, J., 1993. Mapping old growth forests on national forest park lands in the Pacific Northwest from remotely sensed data. Photogrammetric Eng. Remote Sensing. 59 (4), 529–535.

Everson, T.M., Van Wilgen, B.W, Everson, C.S., 1988. Adaptation of a model for fire danger rating in the Natal Drakensberg. South Afr. J. Sci. 84, 44–49.

Finney, M.A., 1999. Mechanistic modelling of landscape fire patterns. In: Mladenoff, D.J., Baker, W.L. (Eds.), Spatial Modelling of Forest Landscape Change: Approaches and Applications. Cambridge University Press, pp. 186–209.

Fons, W.L., 1946. Analysis of fire spread in light forest fuels. J. Agri. Res. 72 (3), 93–121.

Goodman P.S., 1982. The dilemma of artificial water points in Mkuze Game Reserve. In Anonymous (1986). Mkuze Game Reserve Management Plan, Appendix 5. Unpublished. Natal Parks Board, Queen Elizabeth Park, Pietermaritzburg.

Goodman P.S., 1990. Soil vegetation and large herbivore relations in Mkuze Game Reserve, Natal. Unpublished PhD thesis, Univ. of the Witwatersrand, Johannesburg.

Green, K., Finney, M., Campbell, J., Weinstein, D., Landrum, V., 1995. Using GIS to predict fire behaviour. Journal of Forestry, pp. 21–25.

Hargrove, W.W., Gardner, R.H., Turner, M.G., Romme, W.H., Despain, D.G., 2000. Simulating fire patterns in heterogeneous landscapes. Ecol. Modelling 135, 243–263.

Karafyllidis, I., Thanailakis, A., 1997. A model for predicting forest fire spreading using cellular automata. Ecol. Modelling 99, 87–97.

Kourtz, P.H., O'Regan, W.G., 1971. A model for a small forest fire…to stimulate burned and burning areas for use in a detection model. For. Sci. 17(2): 163–169.

Kushla, J.D., Ripple, W.J., 1997. The role of terrain in a fire mosaic of a temperate coniferous forest. Forest Ecol. Management 96, 97–107.

Luke, R.H., Mcarthur, A.G., 1978. Bushfires in Australia. Australian Government Publishing Service, Canberra, p. 359.

Nelson, R.M., Adkins, C.W., 1986. Flame characteristics of wind-driven surface fires. Can. J. For. Res. 16, 1293–1300.

Nelson, R.M., Adkins, C.W., 1987. A dimensionless correlation for the spread of wind-driven fires. Can. J. For. Res. 18, 391–397.

Putnam A., 1965. A model study of wind-blown free-burning fires. In: Proceedings 14th Symposium on Combustion. Comb. Inst., Pittsburgh. pp. 1039–1046.

Rothermel, R.C., 1972. A mathematical model for predicting fire spread in wildland fuels. USDA For. Serv., Intermt For. and Range Exp. Stn, Ogden, UT. Res. Pap. INT-1 15: pp. 40.

Thompson, M.W., 1993. Quantitative biomass monitoring and fire severity mapping techniques in savanna environments using Landsat Thematic Mapper imager. C.S.I.R. Div. of For. Sci. and Tech. Rep. FOR-DEA 587: pp. 55.

Trollope, W.J., 1978. Fire behaviour—A preliminary study. Proc. Grassland Soc. Southern Afr. 13, 123–128.

Trollope, W.J., 1984a. Fire in savanna. In: Booysen, P., de, V., Tainton, N.M. (Eds.), Ecological Effects of Fire in South African Ecosystems. Springer-Verlag, Berlin, pp. 149–176.

Trollope, W.J., 1984b. Fire behaviour. In: Booysen, P., de, V., Tainton, N.M. (Eds.), Ecological Effects of Fire in South African Ecosystems. Springer-Verlag, Berlin, pp. 199–218.

Von Neumann, J., 1966. Theory of self-reproducing automata. University of Illinois, Urban.

Weise, D.R, Biging, G.S., 1996. Effects of wind velocity and slope on flame properties. Can. J. For. Res. 26, 1849–1858.

Weise, D.R., Biging, G.S., 1997. A qualitative comparison of fire spread models incorporating wind and slope effects. For. Sci. 43 (2), 170–180.

Wills, A.J., 1987. The "BEHAVE" fire behaviour prediction and fuel modelling system. Unpublished, Natal Parks Board Rep. pp. 23.